N94-33310

POINTING AND TRACKING SPACE MECHANISM FOR LASER COMMUNICATION

A. Brunschvig and M. de Boisanger
Automatic Control Systems & Propulsion Division
Matra Marconi Space
Toulouse, France

ABSTRACT

Space optical communication is considered a promising technology regarding its high data rate and confidentiality capabilities. However, it requires today complex satellite systems involving highly accurate mechanisms.

This paper aims to highlight the stringent requirements which had to be fulfilled for such a mechanism, the way an existing design has been adapted to meet these requirements and the main technical difficulties which have been overcome thanks to extensive development tests throughout the C/D phase initiated in 1991. The expected on-orbit performance of this mechanism is also presented.

INTRODUCTION

The "Coarse Pointing Assembly" (CPA) is a two-axis gimbals mechanism developed by MMS in the frame of the SILEX (Semiconductor Intersatellite Link EXperiment) ESA program dedicated to optical space communications between Low Earth Orbit and Geostationary Orbit satellites. The first SILEX Terminal is to be flown on SPOT4 LEO spacecraft and its GEO counterpart will be installed on ARTEMIS platform from Alenia. These two Terminals should thus enable the first inter-orbit communication link to be demonstrated in 1997.

To date, a complete flight-representative CPA has been manufactured and qualification of the design has been started. As part of the Pointing, Acquisition and Tracking sub-system, the main function of the CPA is to perform the pointing of the SILEX telescope over wide angles in order to compensate for the satellite ephemerids (see Figure 1).

The SILEX CPA design concept is derived from the IOC (Inter-Orbit Communication) experiment which proved to work satisfactorily on-orbit during the one year flight of the EURECA (EUropean REtrievable CArrier) mission. However, the IOC design which was intended for RF communications has had to be largely adapted to the SILEX specific and more demanding laser communication application.

SYSTEM REQUIREMENTS

The on-orbit mission of the CPA can be split in two distinct phases. The first one corresponds to the "acquisition" of the laser communication beam between the two Terminals each time the LEO satellite comes "in-sight" of the GEO spacecraft.

During this phase, the overall SILEX system operates in open-loop and the CPA must guarantee very accurate and stable pointing of the two telescopes towards each other until the "fine" stage of each Terminal acquires the narrow laser beam. The acquisition procedure involves a particular scanning pattern of the laser beam generated by the GEO satellite beacon over the "uncertainty cone" of the LEO satellite relative position. Because of its open-loop nature, the acquisition phase is the most critical period of the SILEX mission. In particular, the CPA performance (bias and short-term stability) is a major contributor to the probability of acquisition success between the two Terminals.

When the "acquisition" procedure is completed and the communication link is established, the overall system is operating in closed-loop, using the laser beam itself as a pointing error signal. During this second phase, the CPA remains commanded in open-loop and must insure tracking of the two Terminals. The CPA performance requirements are somewhat less critical in this mode regarding pointing accuracy, but a major constraint remains on the torque disturbances induced by the CPA on the host spacecraft. Indeed, these disturbances must be reduced to a minimum in order not to corrupt the satellite payload operations.

The CPA main performance requirements are summarized hereafter :

• Terminal mobile part characteristics :	
- mass	75 kg
- inertia	5 m^2.kg
- mass unbalance	60 mm
• kinematics requirements (2 axes) :	
- angular coverage	< 200 °
- angular rates	< 0.2 °/s
- angular accelerations	< 0.02 °/s^2
• pointing requirements :	
- two-axis bias	< 0.02 °
- two-axis random (f > 0.01 Hz)	< 0.02 ° (3 sigma)
- stability over 1 s (one axis)	< 0.003 °
- stability over 70 ms (one axis)	< 0.001 °
• torque disturbances :	
- torque noise (one axis)	< 2.10^{-8} $(N.m)^2$/Hz (PSD)

DESIGN HERITAGE AND ADAPTATIONS

The CPA is composed of the mechanism itself (CPM) and a dedicated electronic unit (CPDE) as shown on Figure 2. The CPM consists of two articulations (CPMA) linked by a carbon fibre reinforced plastic (CFRP) L-shaped bracket and corresponds to a 800 mm large sub-assembly, weighing 21 kg and dissipating approximately 20 W.

Each CPMA (see Figure 3) features a high resolution hybrid stepper motor mounted on a large annular pre-loaded ball-bearing pair, a direct drive transmission, a 10-bit optical encoder for "coarse" position telemetry, a friction-type blocking device which guarantees stable unpowered position of the telescope, electrical limit stops and a cable-wrap which routes all signals from the Terminal mobile part to the

satellite fixed part with minimum torque disturbances. The CPDE is a fully redundant unit which contains 11 double-Europe size PCB's and two DC/DC converters directly bolted to the box structure. It weighs 12 kg and dissipates a maximum of 30 W.

The motor command is of the open-loop type and uses high resolution micro-stepping technique associated to a high performance current-controlled drive electronics. In order to minimize torque disturbances and pointing errors, models of the main articulation "parasitic" torque (motor, ball-bearings, cable-wrap) are implemented in the electronics processor unit, thus enabling open-loop compensations specific to each CPMA.

Since a significant improvement in performance was required for SILEX with respect to IOC application, the CPA early design phase was mainly devoted to optimizing the original IOC concept. Potential improvements have been investigated in three directions : the articulation design itself, the open-loop compensations and the drive electronics.

In order to reduce the torque noise of the CPMA which cannot be compensated for, it was decided to modify the motor/bearing assembly so that only one bearing pair would be implemented instead of two, as for IOC. This modification was compatible with the SILEX specified launch loads. The other major design change which was identified to reduce further the bearing torque noise was a change in lubrication. The CPMA design was adapted to accommodate wet lubricant which was felt to induce smoother motion capability than solid MoS_2 used on IOC mechanism. Finally, the teflon individual ball separators were replaced by phenolic retainers which were also considered a better solution for torque regularity, especially during transitions at change of motion direction.

Based on IOC experience, the articulation model was reviewed and the open-loop compensations of the CPMA "parasitic" torque have been refined and adapted to match more closely the specific SILEX needs.

Regarding the motor driver electronics, the topology of the IOC power amplifiers (PWM type) has been largely modified in order to improve the motor current accuracy and the related harmonic distortion which generates torque disturbances.

PERFORMANCE-DESIGN RELATIONSHIP

The overall CPA pointing performance stems from one axis performance which is combined at the two-axis level, taking into account the L-bracket influence.

The one axis bias is directly influenced by the mean resistive torque of the CPMA which is composed of :

- bearing/motor overall solid friction torque (hysteresis),
- bearing/motor equivalent viscous friction torque,
- cable-wrap stiffness and hysteresis.

The final pointing bias performance is determined by the on-ground compensation residuals of these resistive torques and by their on-orbit environmental and aging effects which are not compensated for (see Figure 4).

L-bracket contributions to the two-axis pointing bias are mainly related to the on-ground misalignment measurement uncertainties, the launch effects (micro-displacements) and to the on-orbit thermoelastic and desorption behavior.

One axis short term stability, random pointing performance and torque disturbances are essentially determined by :

- torque harmonics (motor, electronics),
- overall torque noise (motor, bearings, electronics) over the relevant frequency range,
- motor transfer function.

The torque harmonics and noise spectra, which are frequency-related to the angular rate of the CPMA, are filtered by the motor transfer function. They are amplified at motor resonance (1.8 Hz, + 20 dB typical). It is of the utmost importance that their initial amplitude be as small as possible. For this reason, initial compensation of the motor harmonics is required. Nevertheless, the motor harmonic compensation residuals will be largely influenced by the CPMA remaining bias error. Indeed, this uncompensated error induces a phase shift in all harmonic compensations, equivalent to an increase of the harmonic residuals (see Figure 5) which, in turns, degrades all dynamic performance.

The LEO dynamic performance (pointing and torque) is more critical, since the LEO kinematics requirements (< 0.2 °/s) are more stringent than the GEO ones (< 0.02 °/s).

Because the final CPA performance would be so closely dependent on the various design adaptations and modifications made after IOC, it was decided to begin validation through extensive development tests on dedicated flight-representative bread-board and engineering models. These tests have involved 3 successive articulations and one electronic unit. They have been mainly oriented towards the following :

- compensation architecture validation,
- bearing assembly performance,
- cable-wrap torque behavior,
- motor harmonics identification,
- drive electronics performance.

COMPENSATION ARCHITECTURE

The CPA overall compensation architecture involves both one axis and two-axis error compensations. The two-axis compensation being purely geometrical (e.g. L-bracket non perpendicularity), it is directly performed by the On-Board-Processor (OBP) which sends the commands to the CPA : actual positions of the rotation axes with respect to the CPA mechanical interfaces are identified on-ground at CPA level and fed to the OBP which can then compute the relevant corrections on each single axis command.

The CPA one axis compensation architecture is described in Figure 6. The OBP angular relative commands are received and processed by the CPDE at 50 Hz. Four initial corrections are computed in parallel and applied to these commands so that the various "parasitic" torques of the articulation can be compensated:

- the motor torque harmonics H_4 (fourth harmonic of the electrical period) which corresponds mainly to the motor detent torque :

$$C_{H4} = C_0 \sin 4p\theta$$

- the articulation overall torque hysteresis Cd represented by a solid friction Dahl model of the form :

$$dC_d = -K_d \left(1 + \text{sign } (d\theta) \frac{C_d}{C_{d_{max}}} \right) d\theta$$

Although this model was known to specifically represent bearing friction behavior [1], its application was extended to include the combination of all CPMA hysteresis sources including the motor and possibly the cable-wrap. For small amplitude alternate angular displacements, this model superimposes an additional equivalent stiffness (K_d) to the motor stiffness. For higher amplitude displacements, torque saturation is reached and the influence on motor stiffness disappears. This behavior was well observed and correlated with the model throughout the development tests.

- the articulation overall viscous resistive torque, proportional to the angular rate :

$$C_v = -F_v * \frac{d\theta}{dt}$$

- the cable-wrap resistive torque induced by its average stiffness :

$$C_{cw} = K_{cw}(\theta - \theta_0)$$

This correction uses the absolute angular position information θ delivered by the 10-bit optical encoder.

The corrected relative angular commands are then used to read the sine and cosine PROM tables which contains 2048 current values over the motor electrical period (1.2 °). These PROM's also incorporate the motor first (H1) and second (H2) torque harmonic compensations.

Final interpolations are made by the CPDE processor to extend the number of micro-steps over one motor period up to 32 768 and to generate commands at 100 Hz in order to minimize the effect of command harmonics generated by the command quantization. Commands are eventually sent to the 12-bit DAC of the motor drive electronics. The torque harmonic disturbance induced by the 100 Hz command rate is then reduced by an analog second order Butterworth filter. Its simple structure allows stable performance and the induced command phase shift can thus be open-loop compensated at OBP level.

For each articulation, these compensation parameters are derived from a specific characterization test procedure which is being carried-out on a dedicated test bench (see Figure 7). This characterization procedure involves specific angular profiles at

different rates and accelerations which are automatically generated and commanded to the articulation.

The test set-up features Kistler piezo sensors for torque measurement and a 24-bit Heidenhain optical encoder for position error determination (static and dynamic). The performance of the motor driver implemented in the test bench are such that the contribution of the electronics to the CPMA pointing errors and torque disturbances is negligible. The same test bench is also used for articulation fine performance verification after compensation.

The above described compensation architecture was successfully tested on the articulation bread-board both without and with cable-wrap.

BEARING ASSEMBLY

The CPA bearing assembly is made of two ball-bearings mounted 40 mm apart on beryllium spacers. Ball-bearings themselves are 200 mm large annular high precision (ABEC 7T) bearings from ADR with phenolic retainers lubricated with Pennzane SHF 2000.

Given the size constraint on the bearing assembly, the main concern is to minimize the ball-bearing mean torque and torque noise. The mean torque induces direct bias on the CPMA pointing accuracy and the torque noise impacts the random budget, the short term stability and torque disturbances.

To reduce the initial bias, the ball-bearing mean torque is characterized on ground for each CPMA at various angular rates in both CW and CCW directions. Its behavior is represented by a viscous friction torque coefficient and a solid friction torque (Dahl model) which is part of the CPDE open-loop compensations. It is then crucial that all variations of this average torque (including torque noise) which cannot be compensated for, be reduced to minimize the on-orbit pointing degradation.

Assuming the bearing torque variations are somewhat proportional to the initial average torque, it was decided to minimize this mean torque in the first place. For that purpose, the initial pre-load adjustment was specified to a minimum (300 N) for this type of bearing and the tolerance on this value was not to exceed ± 30 N. The first development tests made on a representative motor/bearing assembly showed an unexpectedly high bearing mean torque which was also not consistent with the test results obtained by the bearing manufacturer. Investigation revealed that the initial pre-load was largely modified after integration of the bearing in the CPMA housing. Machining tolerances would not allow the radial bearing expansion during the clamping operation. After detailed calculation and measurements (see Figure 8) of the typical expansion of the inner and outer rings, each CPMA housing has been matched to the bearing actual dimensions to accommodate this expansion effect and to minimize the residual clearance after clamping which could generate transverse bias of the CPMA rotation axis.

A major source of on-orbit pre-load variation is the thermal environment of the mechanism which can induce temperature gradients between inner and outer rings

of the bearing. Based on IOC bearing conductance data, preliminary thermal analysis showed that the maximum expected temperature gradient on the bearing would be such that the initial small pre-load could be entirely lost, thus leading to unacceptable transverse bias of the CPMA rotation axis. Yet, it was felt that the change in lubrication could have a significant impact on this result for SILEX. Additional tests confirmed that the bearing conductance was indeed significantly improved by the presence of wet lubrication and was very little affected by the pre-load itself or the lubricant exact quantity. The refined thermal analyses predicted temperature gradients of less than -2 °C/+1.5 °C.

Under such circumstances, theoretical bearing analyses showed that the worst case pre-load variations induced by thermoelastic effects (see Figure 9) would be acceptable.

After the initial bearing pre-load and its variations had been validated, the relationship between the mean torque and these pre-load variations were measured (see Figure 10). It was thus demonstrated that the bearing mean torque would remain below 0.03 Nm for the CPA application (rates < 0.2°/s). Torque noise itself was not precisely measured during these tests but it was considered not to exceed 0.003 Nm over the entire pre-load range. This hypothesis would be confirmed later-on during CPMA performance tests.

Considering the stringent CPA two-axis bias and random specifications, it is also very important that the transverse articulation pointing errors be minimized. These errors, known as the wobble (mean value and noise), are essentially determined by the bearing, spacer and housing geometrical imperfections after assembly. Because of significant volume constraints, the CPA bearing assembly overall implementation was not optimized with respect to such errors. Indeed, the small distance imposed between the two large annular bearings make the design very sensitive to these geometrical imperfections. In order to minimize this effect, most parts involved in the bearing assembly have been machined with an accuracy down to 3 µm. Resulting wobble figures on the order of 10 arcsec for average values and of 5 arcsec for noise have been consistently measured.

CABLE-WRAP

The cable-wrap resistive torque behavior over the CPMA angular coverage would induce both pointing errors and torque disturbances. Indeed, the overall cable-wrap stiffness and hysteresis would generate a variable pointing bias of the CPMA which in turns would degrade the motor harmonic compensations and therefore the dynamic performance. For that reason, the compensation architecture within the CPDE foresees the compensation of the cable-wrap stiffness and hysteresis on the basis of on-ground characterization.

The exact behavior of the cable-wrap resistive torque is closely dependent on the actual technology used for the sheet manufacturing, the definition and the number of cables implemented, the detailed design of the attachment points and the sheet geometry. Final performance of the cable-wrap were therefore difficult to predict and

it was decided that the main design trade-offs should be shortly followed by development tests on a flight-representative cable-wrap bread-board.

The overall cable-wrap behavior was characterized both at ambient and extreme temperatures. It appeared that the stiffness variation over the temperature range was small enough (<35%) that no compensation versus temperature was needed. The hysteresis behavior however was significantly different than what was anticipated. The absolute value of the hysteresis was higher than expected and the hysteresis pattern was also such that the transitions at change of direction were fairly "slow" (over 20 ° typical), thus reducing the linear portions of the cycle (see Figure 11) and making the average stiffness estimation less accurate.

The origin of this observation could be two-fold : the sheet plastic deformation itself and the friction of the sheets on the bottom of the cable-wrap structure under the influence of gravity. A new test simulating "0G" on-orbit conditions showed that the friction phenomenon contributed to only 10 % of the overall hysteresis. On-ground characterization of the cable-wrap hysteresis was therefore not questioned. Identification of the bearing/motor solid friction torque for compensation purposes would not be corrupted by the parasitic friction of the cable-wrap ("0G" test not practical on flight hardware).

Nevertheless, the "soft" transitions observed on the hysteresis cycle were no longer compatible with the compensation pattern foreseen in the CPDE (single Dahl model for all hysteresis sources). It was shown that the actual behavior of the cable-wrap torque hysteresis could be well described by a specific Dahl model with reduced equivalent stiffness (K_d). However, implementation of a second Dahl model in the compensation architecture has not been decided yet.

The CPA pointing budget has been consolidated assuming no specific compensation of the cable-wrap hysteresis and assuming its origin is pure plastic behavior of the sheets. Additional aging and thermal uncompensated effects (±50 %) are therefore applied to the total measured hysteresis in order to derive worst case end-of-life figures.

MOTOR HARMONICS

Based on IOC experience, it was known that, for this type of motor (SAGEM 57PPP60), the torque harmonics H_1, H_2 and H_4 of the electrical period were the most significant in amplitude and could be well identified and compensated for. Higher harmonics were shown to be also highly unstable, both in amplitude and phase, over a complete motor revolution. Compensation efficiency of these harmonics would therefore be rather poor.

Nevertheless, motor harmonics are identified for each articulation up to the 12th harmonic. Amplitudes and phases are determined from the pointing error measured under quasi-static conditions (no dynamic effects involved) over 15 ° coverage selected around the cable-wrap mid-point, using a least square identification algorithm. The compensation efficiency is then verified over the complete CPMA

angular coverage and iterations can be made to optimize the final parameters. Figures better than 70% have been achieved on-ground for H_1, H_2 and H_4 compensation efficiency. Worst-case on-orbit performance should be better than 50%.

As the highest contributor to dynamic pointing errors and torque disturbances, the compensation of H_4 harmonic is very critical and requires particular attention. For that purpose, the phase of H_4 is identified specifically for each direction of the motor rotation whereas a single phase (average value) is determined for each harmonic H_1 and H_2, regardless of the direction of motion. It was further verified that H_4 amplitude before compensation was almost not affected (< 5 %) by the temperature variations of the motor itself or the maximum amplitude of the current driven into the motor phases. The compensation of H_4 would therefore be fairly robust to the motor direct environment.

DRIVE ELECTRONICS

Particular attention has been paid to the drive electronics imperfections so that their impacts on the overall CPA performance be minimized. The main end-of-life requirements applicable to the CPDE are the following :

- amplifier gain asymmetry: < 0.4 %
- current offset asymmetry : < 0.4 % of max amplitude
- current settling time asymmetry : < ± 3 ms
- current noise : < 50 µA/ $\sqrt{Hz}$ (PSD)
- harmonic distortion : > 74 dB

Development test results have been successfully correlated with the theoretical analyses which showed that the CPDE current offset asymmetry between phases directly generates H_1 harmonic and that amplifier gain error as well as settling time asymmetry actually create H_2 harmonic.

CPDE specifications were established in such a way that H_1 and H_2 harmonics generated end-of-life by the electronics would be of similar amplitude to H_1 and H_2 motor harmonics, after compensation. Current noise and harmonic distortion stringent requirements would also guarantee that the beginning-of-life CPDE contribution to the CPA random and stability budgets be less important than the motor/bearing effect.

Compatibility tests with a CPMA bread-board have confirmed that the beginning-of-life CPDE performance were much better than the specifications and that the CPMA compensations were not affected by the electronics. This result justified a posteriori that the identification of the compensation parameters for each CPMA model could be performed without the associated CPDE. The resulting programmatic flexibility would be exploited.

CPA PERFORMANCE

Because of the high pointing accuracy and stability required from the CPA, verification of the two-axis performance by test was rapidly found not to be practical. Indeed, the influence of gravity would induce pointing errors one order of magnitude higher than those to be measured. Furthermore, these errors would vary significantly over the specified CPA wide angular coverage and their compensation would be very complex (e.g. anti-gravity device).

The selected approach for performance verification was therefore to extensively focus on the one axis performance measurements at the CPMA level and to rely on a detailed one axis functional simulation model and a theoretical pointing budget in order to extrapolate the two-axis worst case CPA performance.

The detailed CPA one axis simulation model which has been developed includes non linear dynamic models of the motor, the bearings, the cable-wrap, the CPDE processor unit with all CPMA compensations and the motor drive electronics. This simulation model was refined and validated throughout the various development tests referred to above. It was then extensively used for test prediction and interpretation, sub-assembly specification analyses, performance assessment during transitions (change of motion direction) and correlation with the linear mathematical model used for the overall CPA pointing budget calculations.

Worst case predictions of one axis performance are then obtained from the mathematical model under steady-state conditions, assuming combined environmental and aging effects (see Figure 12 for results). Torque noise performance was directly derived from bread-board measurements which typically exhibited low-frequency noise spectra (<1 Hz) at an angular rate of 0.2 °/s. Computation of the equivalent PSD ($5\ 10^{-5}$ $(Nm)^2/Hz$) from the total variance shows that it remains a very critical performance with respect to the requirements.

The individual azimuth and elevation pointing errors are then combined at two-axis level, taking into account their probability distributions. L-bracket contributions such as initial misalignment measurement uncertainties, thermoelastic and desorption effects (calculated) are also superimposed to extrapolate the final two-axis CPA performance. Only the structural dynamic behavior of the L-bracket is not taken into account in the CPA two-axis performance presented in Figure 13. This contribution is analyzed and consolidated at system level within the overall SILEX Terminal pointing budget.

CONCLUSION

The CPA illustrates the ability of a large open-loop mechanism to meet high dynamic pointing accuracy and reduced torque disturbances. This performance have been achieved thanks to detailed characterization and fine tuning of the design, thus enabling the definition of efficient open-loop torque compensations. The importance of development tests on flight-representative hardware in this context has been emphasized.

It should be considered, however, that the ultimate performance has been reached for this type of mechanism using open-loop technology. Closed-loop design would be recommended to meet even more stringent requirements or to provide better evolution potentials.

REFERENCES

[1] Models for steady & non steady Coulomb Torque in Ball-bearings, M.J. Todd, ESTL Northern Research Lab., Risley, England

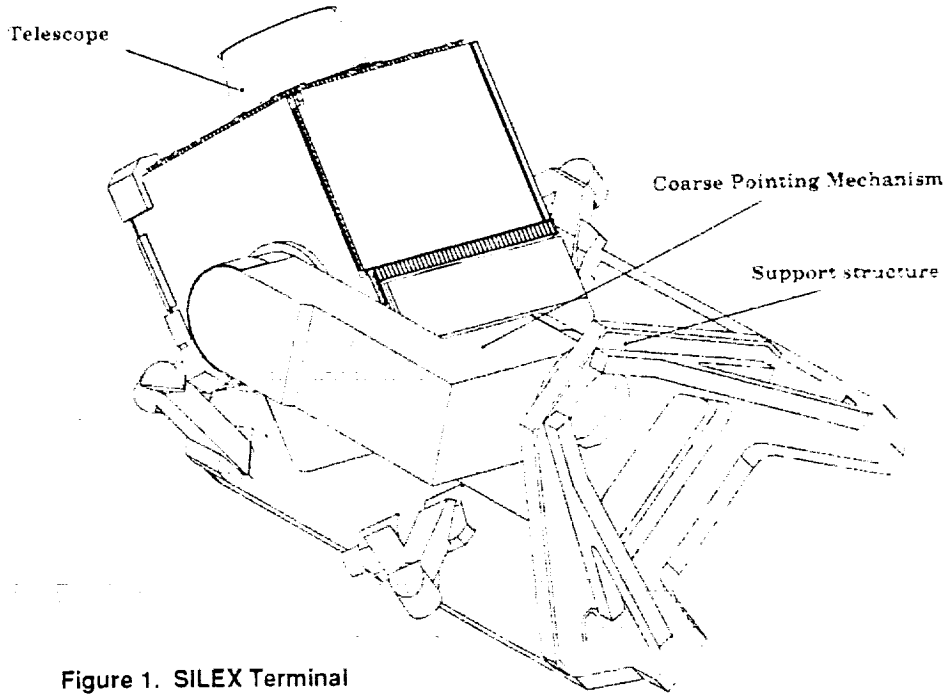

Figure 1. SILEX Terminal

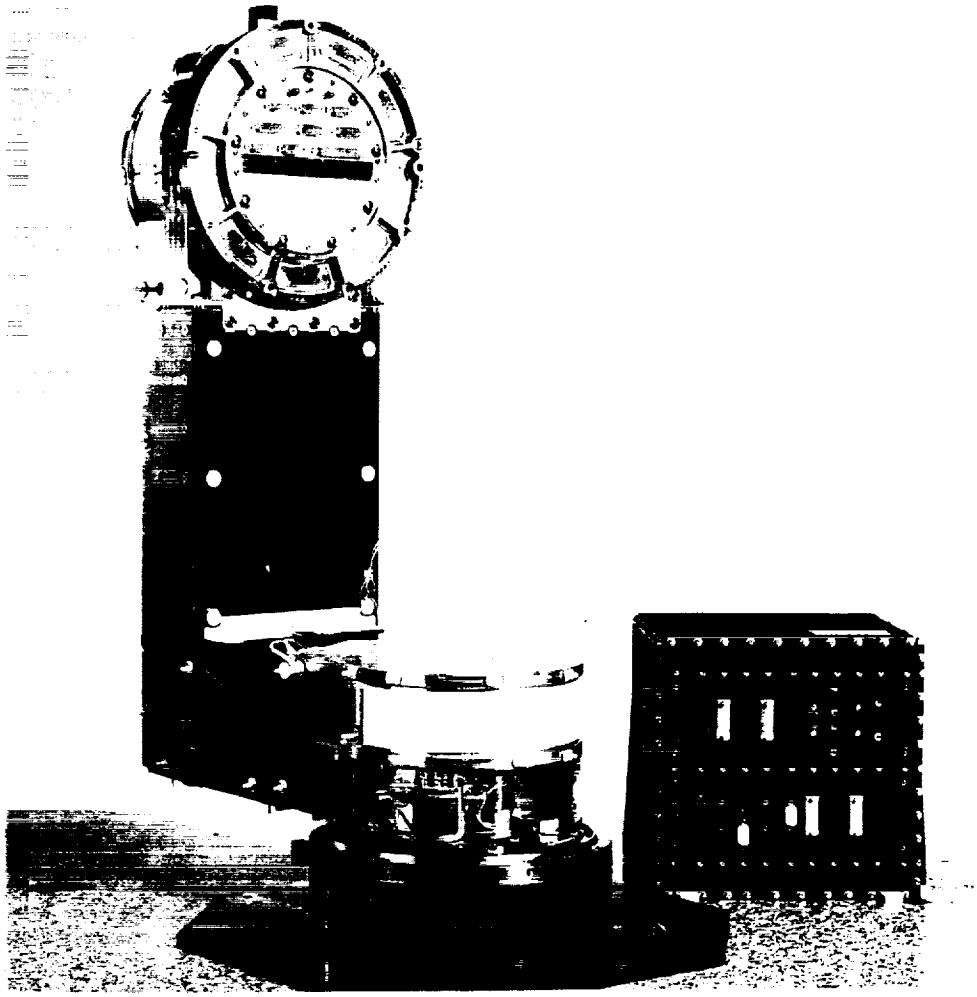

Figure 2. CPA (flight representative)

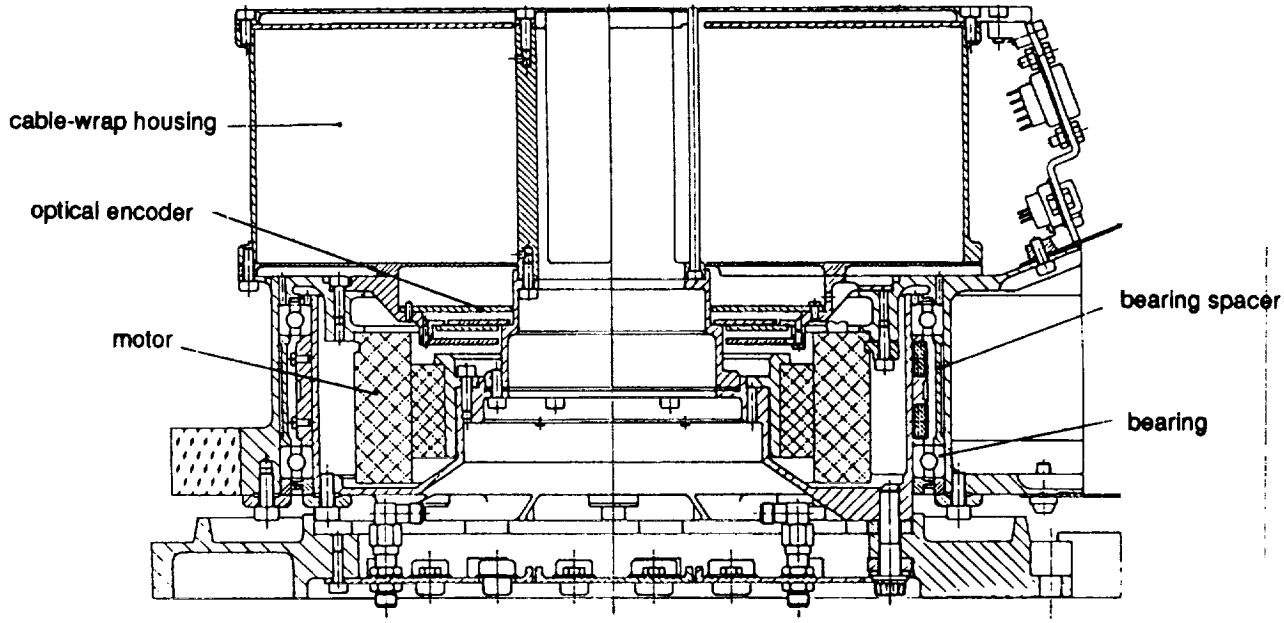

Figure 3. CPMA cross-section

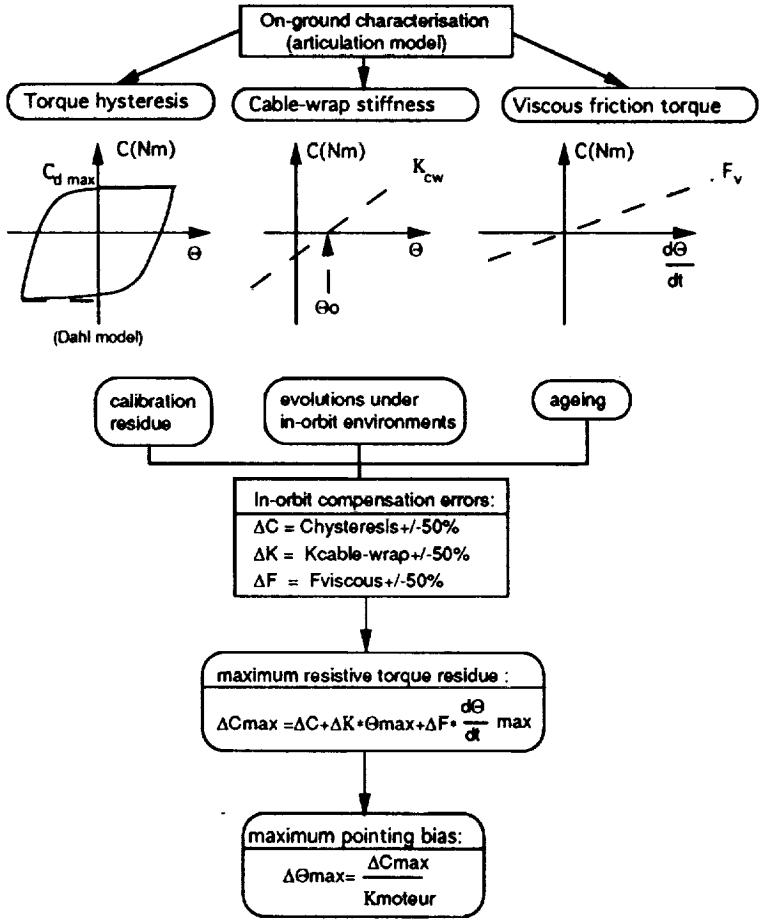

Figure 4. Estimation of maximum in-orbit pointing bias (one axis)

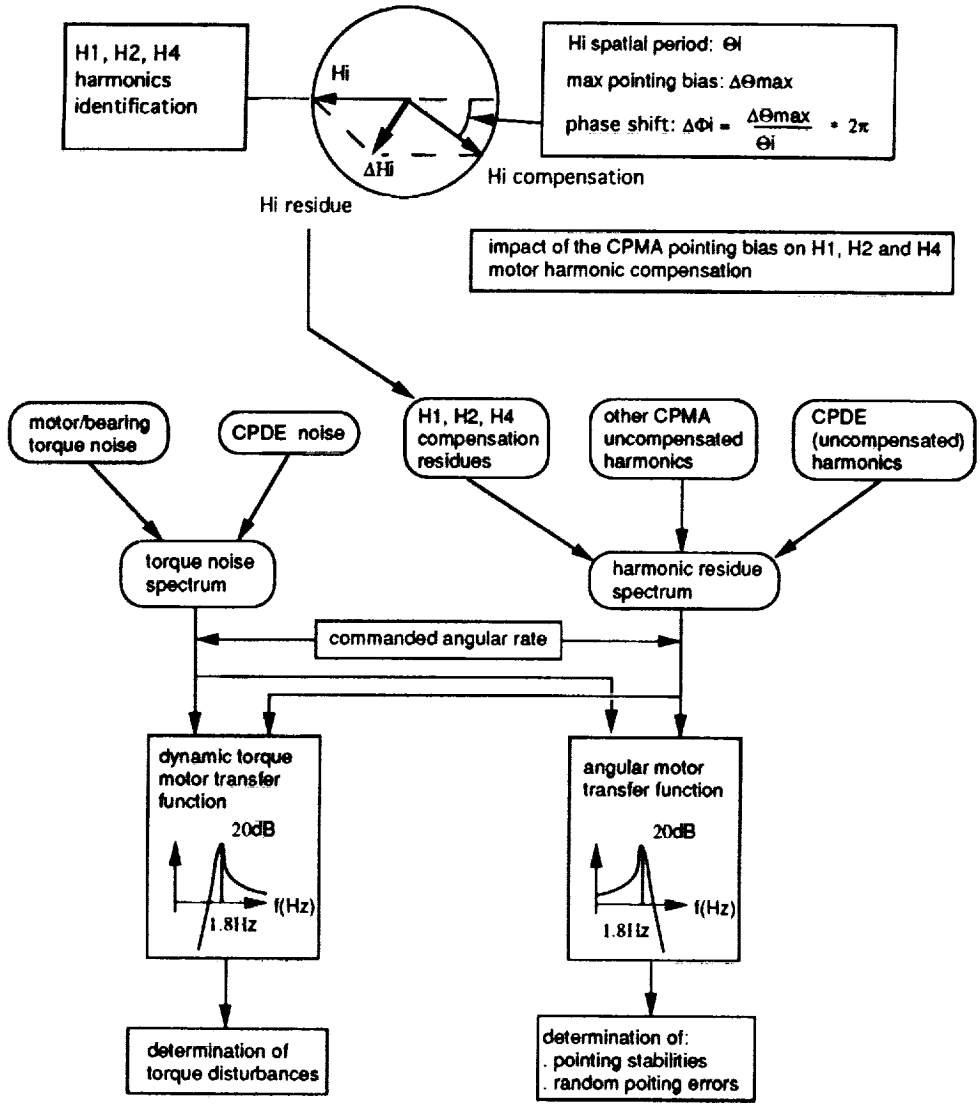

Figure 5. Torque harmonics and torque noise impacts on dynamic performances (one-axis)

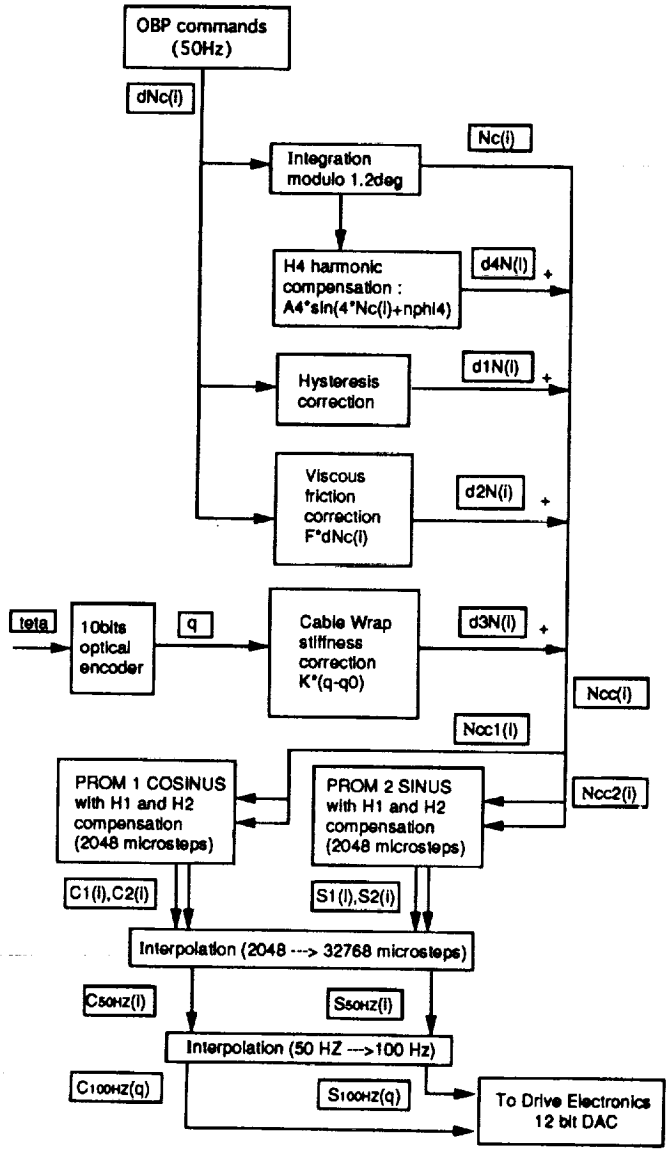

Figure 6. Compensation architecture

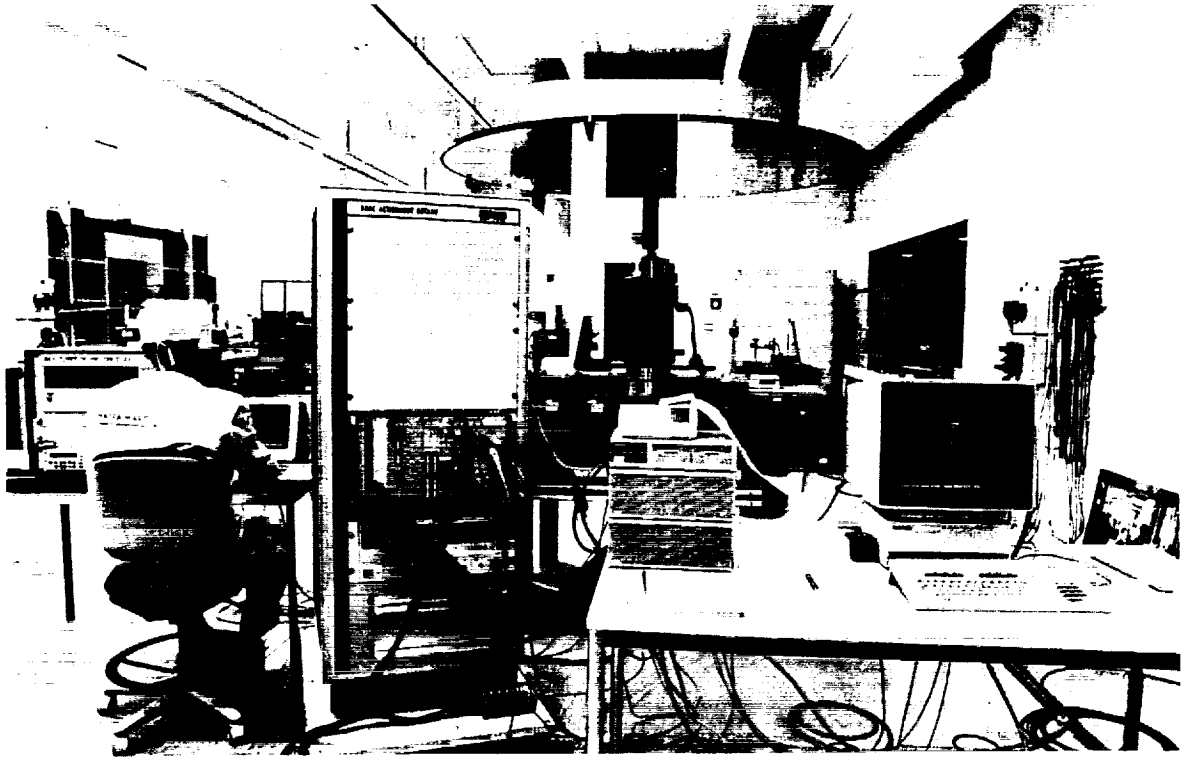

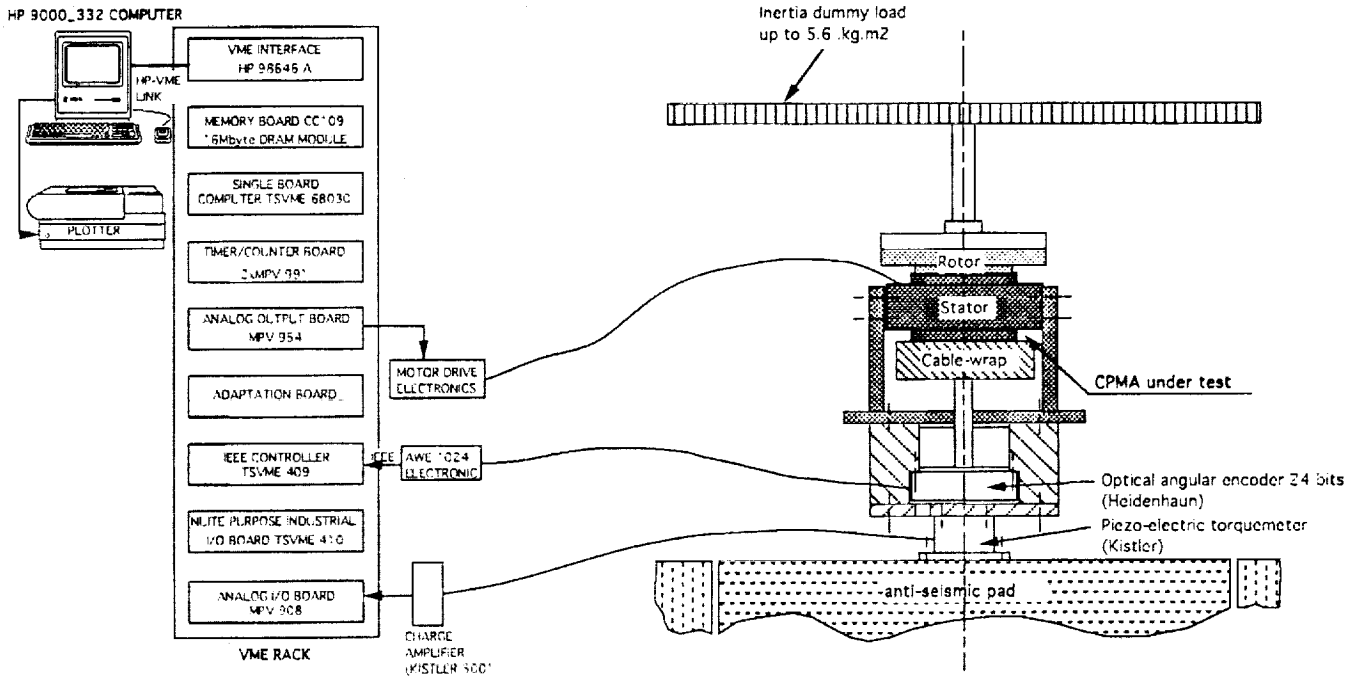

Figure 7. CPMA Test bench

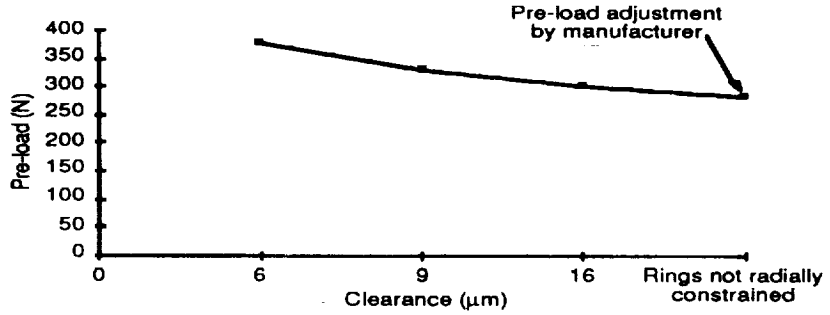

Figure 8. Bearing pre-load vs outer-ring/housing clearance (measured)

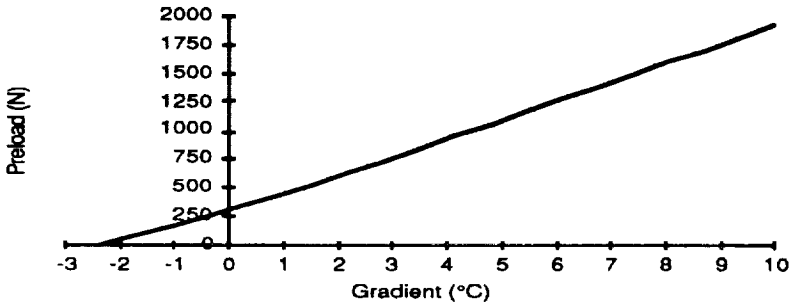

Figure 9. Bearing pre-load vs temperature gradient (calculated)

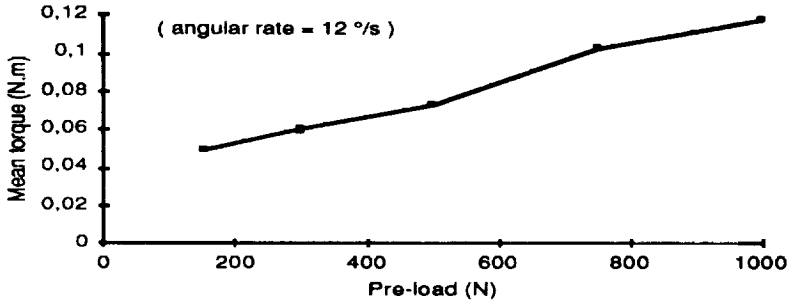

Figure 10. Bearing mean torque vs pre-load (measured)

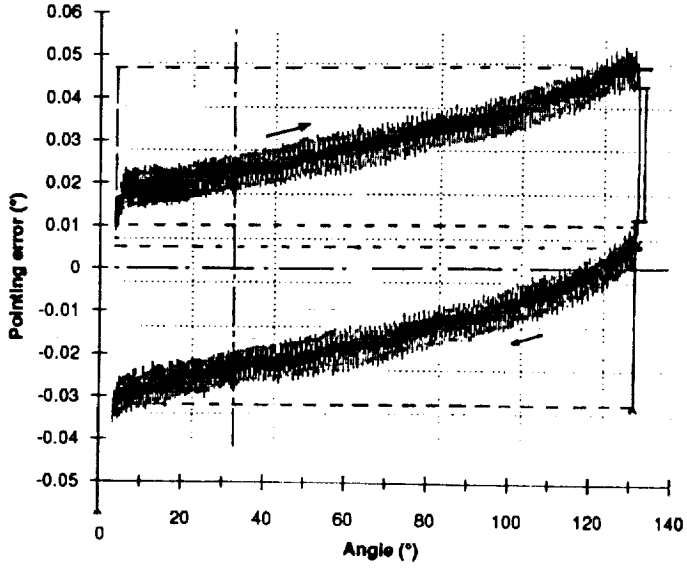

Figure 11. Typical CPMA pointing error hysteresis

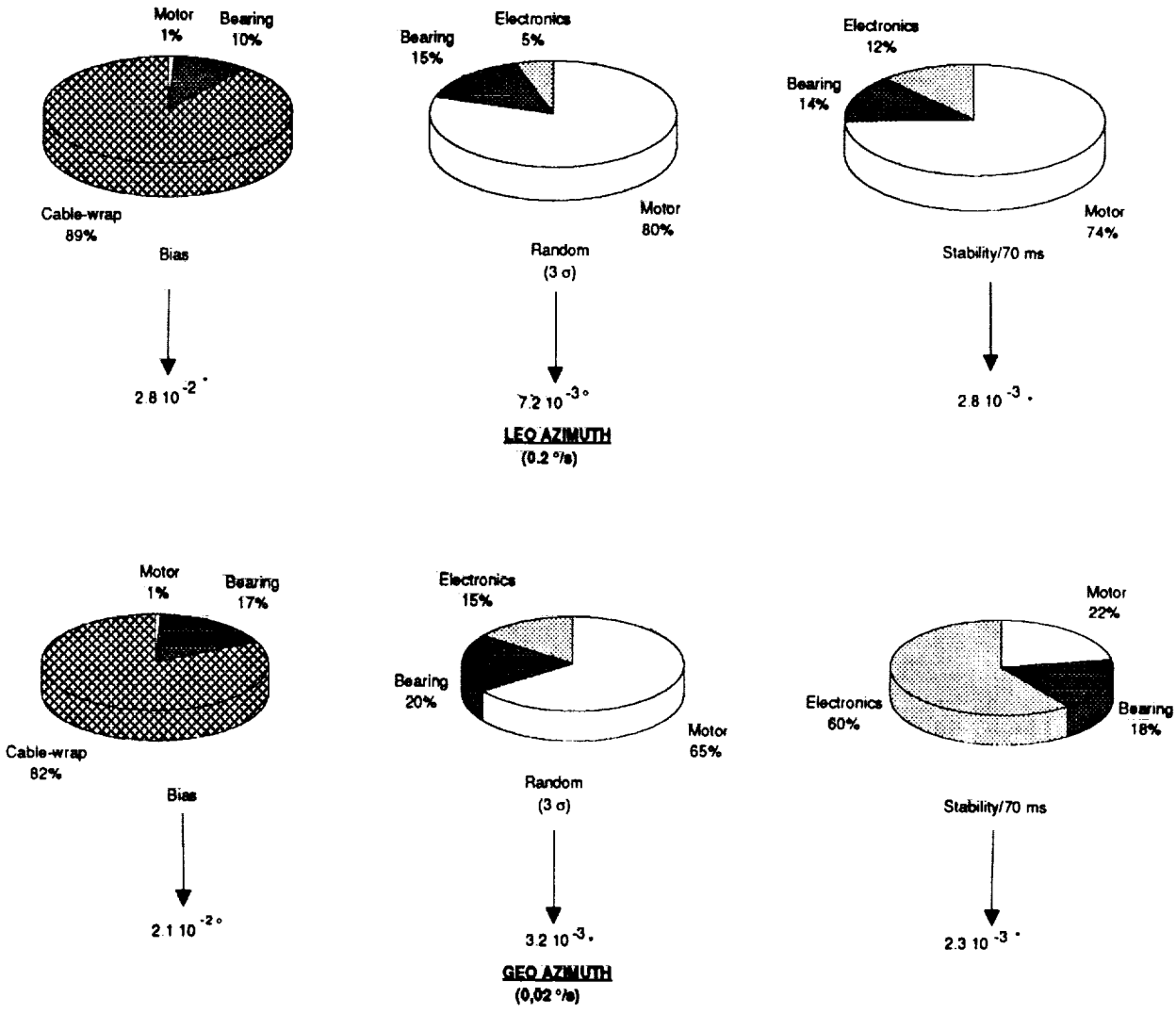

Figure 12. One axis worst-case pointing performances with contributors identification

	LEO (0,2 °/s)	GEO (0,02 °/s)
Bias	$3{,}2\ 10^{-2}$ °	$2{,}8\ 10^{-2}$ °
Random (3 σ)	$8{,}0\ 10^{-3}$ °	$4{,}0\ 10^{-3}$ °

Figure 13. Two-axis worst-case pointing performances